ELSEVIER

Clinical Neurophysiology 112 (2001) 545–550

www.elsevier.com/locate/clinph

A convenient method for detecting electrolyte bridges in multichannel electroencephalogram and event-related potential recordings

Craig E. Tenke*, Jürgen Kayser

Department of Biopsychology, Unit 50, New York State Psychiatric Institute, 1051 Riverside Drive, New York, NY, USA

Accepted 4 December 2000

Abstract

Dense electrode arrays offer numerous advantages over single channel electroencephalogram/event-related potential (EEG/ERP) recordings, but also exaggerate the influence of common error sources arising from the preparation of scalp placements. Even with conventional low density recordings (e.g. 30-channel Electro-Cap), over-application of electrode gel may result in electrolyte leakage and create low impedance bridges, particularly at vertically-aligned sites (e.g. inferior-lateral). The ensuing electrical short produces an artificial similarity of ERPs at neighboring sites that distorts the ERP topography. This artifact is not immediately apparent in group averages, and may even go undetected after visual inspection of the individual ERP waveforms. Besides adding noise variance to the topography, this error source also has the capacity to introduce systematic, localized artifacts (e.g. add or remove evidence of lateralized activity). Electrolyte bridges causing these artifacts can be easily detected by a simple variant of the Hjorth algorithm (intrinsic Hjorth), in which spatial interelectrode distances are replaced by an electrical analog of distance (i.e. the variances of the difference waveforms for all pairwise combinations of electrodes). When a low impedance bridge exists, the Hjorth algorithm identifies all affected sites as flat lines that are readily distinguishable from Hjorth waveforms at unbridged electrodes.

Keywords: Electroencephalogram; Event-related potential; Methodology; Electrolyte bridge; Dense electrode array; Intrinsic Hjorth

1. Introduction

The scalp topographies of electrophysiologic measures (e.g. alpha power, P300 amplitude), which are derived from the raw electroencephalogram (EEG) or from event-related potentials (ERP), are frequently used to identify, localize, and compare the regional patterns of neuronal activation associated with different experimental conditions (e.g. Picton et al., 2000). Technological advances have substantially improved the spatial resolution of these scalp topographies by using closely spaced electrode montages (e.g. Tucker, 1993). The localizing capacity of these methods has been further enhanced by the use of various mathematical transformations (e.g. surface Laplacian) to sharpen topographies (e.g. Perrin et al., 1989; Gevins, 1996). However, conventional methods for placing scalp electrodes impose technical limitations on the maximum spatial density of electrodes in any montage (Pellouchoud et al., 1997).

The usefulness of topographic methods relies on the accurate measurement of subtle differences in scalp potentials between nearby electrode sites. Sufficient electrode connectivity to the scalp demands low electrode impedances, which are affected by a number of individual differences, such as hair texture or scalp dryness. During the preparation of scalp recording sites, impedances are therefore commonly reduced to the lowest values that are practical (between 2 and 10 kΩ; cf. Picton et al., 2000) and are typically measured in series with the parallel (linked) impedance of all other sites or a series of adjacent sites in the montage. This prevents the detection of exceptionally *low* impedance values between adjacent electrodes.

Low impedance bridges may result from several identifiable causes. Electrolyte leakage may follow the overapplication of electrode gel, particularly at vertically-aligned sites (e.g. inferior sites on posterior and lateral surfaces of the scalp). However, a bridge between electrodes may also result from problems unrelated to the electrode/scalp interface. An electrical short among the fine lead wires within a connector cable, or erroneous jumper connections in the hardware configuration, may effectively bridge scalp sites regardless of their actual scalp locations. The identifying characteristic of a low impedance bridge is the erroneous similarity or identity of electrical activity at the affected sites. The unaided detection of such spurious identities is

* Corresponding author. Tel.: +1-212-543-5483; fax: +1-212-543-6540.
E-mail address: tenkecr@pi.cpmc.columbia.edu (C.E. Tenke).

1388-2457/01/$ - see front matter
CLINPH 2000137
PII: S1388-2457(00)00553-8

difficult even with comparably small 30-channel montages, and becomes considerably more difficult with dense electrode arrays. Although low impedance bridges are more likely with higher electrode density, the overall topographic distortion attributable to any single bridge is proportionately smaller. Electrophysiologists do not commonly examine individual ERP waveforms for these artifacts, and incidental discoveries during routine visual inspection are unlikely when focusing on dorsal and midline sites, where classical ERP components are largest. The ultimate impact of such electrolyte bridges on group averages can range from a subtle, unpredictable smearing of localized effects (i.e. adding noise variance to the topography), to the introduction of systematic, localized artifacts, resulting, for example, in an erroneous insertion or attenuation of small hemispheric asymmetries.

A simple mathematical transformation of the ERP waveforms can provide an easy, objective, and reference-independent method for identifying electrolyte bridges. We illustrate below the fortuitous properties of the intrinsic Hjorth (NeuroScan, 1995), a simple variant of the Hjorth Laplacian algorithm in which the variance of the potential difference between electrodes is substituted for spatial distance between them, with real and simulated 30- and 129-channel data. Although not previously used for this purpose, it is suggested that an improved implementation of the intrinsic Hjorth algorithm will effectively detect bridged electrodes in EEG and ERP data.

2. Methods

2.1. Hjorth Laplacian

The Hjorth algorithm (Hjorth, 1980) is a method of computing a linear approximation of the surface Laplacian. The Hjorth waveform $H_i(t,N)$ represents the contribution of the signal at each electrode i as the difference between the time-varying potential $P_i(t)$ and the scaled sum of the potentials $P_j(t)$ at each of N neighboring electrodes

$$H_i(t,N) = P_i(t) - \sum_{j=1}^{N} P_j(t) W_{i-j}(N) \quad (1)$$

where the weighting factor W_{i-j} for each neighbor is proportional to the inverse of the distance d_{i-j} between the electrodes

$$W_{i-j}(N) = \frac{1/d_{i-j}}{\sum_{k=1}^{N} (1/d_{i-k})} \quad (2)$$

This algorithm may be generalized to include any number of neighboring electrodes.

2.2. Intrinsic Hjorth

The intrinsic Hjorth, originally a 'beta' feature of NeuroScan's EDIT module (version 3; NeuroScan, 1993), is a variation of the Hjorth Laplacian in which spatial distance is replaced by a nonspatial 'electrical distance' measure reflecting the electrical similarity of electrodes (NeuroScan, 1995). For any pair of electrodes i and j, a potential difference waveform $P_{i-j}(t)$ may be computed as

$$P_{i-j}(t) = P_i(t) - P_j(t) \quad (3)$$

The 'electrical distance' measure D_{i-j} is defined as the temporal variance[1] of the difference potential waveform

$$D_{i-j} = \frac{1}{T} \sum_{t=1}^{T} (P_{i-j}(t) - \overline{P_{i-j}(t)})^2 \quad (4)$$

The intrinsic Hjorth is produced by replacing d_{i-j} of Eq. 2 with D_{i-j}. In the case of a single neighbor, the intrinsic Hjorth waveform is identical to the difference potential $P_{i-j}(t)$ for the nearest neighbors given by D_{i-j}. Since the intrinsic Hjorth waveforms converge to zero as any D_{i-j} approaches zero (i.e. $W_{i-j}(t)$converges to one as the numerator and denominator of Eq. 2 converge[2] they will be distinct from all other channels whenever two electrodes are bridged.

For a montage consisting of M recording electrodes, an $M \times M$ matrix of electrical distances D_{i-j} may be computed. For each electrode, the electrical distances to each other electrode are ranked to determine the N nearest electrical neighbors. However, since this application is only intended to determine whether any given electrode is bridged to another electrode or not, it is sufficient to restrict the analysis to the detection of the single nearest *electrical* neighbor (i.e. $N = 1$ in Eq. 1).[3]

2.3. Physiological recordings

Sample EEG/ERP data were recorded with a 30-channel electrode cap (Electro-Cap International, Inc.) and a 129-

[1] because a volume conducted signal changes linearly over distance if no local generator is present, i.e. the second spatial derivative is zero (Mitzdorf, 1985), the standard deviation, which also varies linearly, would provide a closer analog for spatial distance. However, the present implementation produces identical results with only one neighbor.

[2] Eq. 2 becomes computationally undefined for $d_{i-j} = 0$. Although measurement noise (e.g. resulting from physical differences between amplifiers) make this condition unlikely for real data, W_{i-j} may be appropriately defined as one for the analogous case in the intrinsic Hjorth (i.e. $D_{i-j} = 0$ when the two waveforms are identical).

[3] In NeuroScan's implementation of the intrinsic Hjorth, the detection of the nearest electrical neighbors is coupled to the production of a transformation matrix used to generate the intrinsic Hjorth waveforms. This *linear derivation* matrix (LDR file) is then applied to the original data. To limit the number of nearest electrical neighbors to $N = 1$, the keyword statement 'CSD_EM_NEIGHBORS 1' must be added to NeuroScan's configuration file (SCAN.CFG). In the (unlikely) case of two precisely identical ERP waveforms, NeuroScan's transformation matrix reflects the mathematically undefined condition of Eq. 2 (i.e. $d_{i-j} = 0$; cf. footnote 2) by printing the error term 'nan' in the affected rows of the matrix (except for the diagonal elements, which correctly hold 1.0). In this case, the transformation matrix (i.e. the LDR file) must be modified by replacing this error term with −1.0 in the column of the paired channel, and with 0.0 in all other columns.

channel Geodesic Sensor Net (Electrical Geodesics, Inc.; Tucker, 1993). Applying standard EEG methodology, data were recorded with Grass amplifiers using a nose reference for the 30-channel data (e.g. Tenke et al., 1998), and with Net Amps (Electrical Geodesics, Inc.) using a vertex reference for the 129-channel data (e.g. Kayser et al., 2000). Interelectrode impedances were maintained below 5 kΩ (Electro-Cap with gel electrolyte; tin electrodes) or 50 kΩ (Sensor Net sponges soaked in KCl; Ag/AgCl electrodes). The recording epoch was 1280 ms (200 ms baseline). Sampling rate was 100 Hz (128 samples/epoch) for the 30-channel data, and 200 Hz (256 samples/epoch) for the 129-channel data. Whereas the epochs of the 30-channel data were not filtered off-line, a 20 Hz low pass (24 dB/octave) was applied to the 129-channel data. ERPs were averaged for correctly detected targets in an auditory oddball task (e.g. Tenke et al., 1998).

2.4. Modeling electrolyte bridges and empirical validation

Electrolyte bridges were introduced between electrodes using two methods: (1) artificially creating salt bridges by applying excessive amounts of electrolyte gel (Electro-Cap) or potassium chloride solution (Sensor Net) to selected scalp regions, however, without establishing direct physical contact among sensors; (2) simulating bridges off-line (Sensor Net montage). Simulated bridges were created between two electrode pairs (one for adjacent sites, one for distant sites) by replacing the integer data for both electrodes of a pair with the mean of the pair, then adding simulated digitizer noise to one channel according to a uniform distribution ranging from −2 to +2 digitizer unit (1 A/D unit = 0.242 μV). In addition, for one bridge simulation, a minimal slow potential ('amplifier') drift was added to one channel as a linear trend ranging from 0 to +0.484 μV (2 A/D units) across the recording epoch. Using both commercial software (NeuroScan) and independently developed software optimized for comparing and visualizing electrical distances, the intrinsic Hjorth was applied to these averaged waveforms for the single nearest electrode (i.e. $N = 1$ neighbor in Eq. 1).

3. Results

Examples for 30- and 129-channel ERP waveforms are presented in Figs. 1 and 2. In the 30-channel example, two adjacent inferior-lateral sites over the left hemisphere (P7, P9) and the three occipital sites (O1, Oz, O2) were bridged by excessive amounts of electrolyte gel. Whereas these bridges are not obvious in the ERP topography (Fig. 1A), they are unambiguous in the intrinsic Hjorth waveforms, which show a decisive, readily identifiable reduction in amplitude at the affected sites (Fig. 1B). For instance, a close examination of the original ERPs reveals that the waveforms at P7 and P9 are nearly identical, whereas those at homologous sites over the right hemisphere (P8, P10) are not. The same applies to the ERPs at occipital sites, which are nevertheless distinct from those at the bridged sites P7 and P9. The inset table (Fig. 1B) indicates the nearest *electrical* neighbor for each electrode, ranked according to the electrical distance between them. Electrodes that are identifiable by flat intrinsic Hjorth waveforms also have the smallest electrical distances (low rank). Comparable results were also observed for 30-channel EEG amplitude spectra.

Similar results were found for the 129-channel Sensor Net. A close inspection of the average-referenced ERP topography may determine the simulated salt bridges, but not without considerable effort (see Fig. 2A). However, despite the more than fourfold increase in the number of waveforms, the simulated bridges at central (adjacent sites: 106/107) and opposite parietal (distant sites: 43/99) sites were likewise unambiguous in the intrinsic Hjorth waveforms (Fig. 2B), yielding low electrical distance values (i.e. 0.002 and 0.024; see inset table in Fig. 2B). Evidence of additional bridges, presumably attributable to the excess of electrolyte solution, was also seen at inferior-lateral sites, showing somewhat larger electrical distance values (between 0.054 and 0.140).

As can be seen from Fig. 2B, the intrinsic Hjorth waveforms of both the simulated bridge at the distant sites 43/99 (which also included a simulated amplifier drift) and of the adjacent sites 56/63 (presumed to be an artificial salt bridge) show evidence of slow potential drifts. To remove these drifts, a linear detrend and a new baseline correction were applied to these ERP waveforms. The intrinsic Hjorth transformation of the corrected ERPs effectively removed the difference between the two simulated bridges (i.e. yielding an electrical distance of 0.002 for both pairs with and without amplifier drift), and clearly reduced the electrical distance values for the adjacent electrode pairs at inferior-lateral sites (i.e. 0.028 for 56/63, 0.054 for 69/70, 0.064 for 95/100).

4. Discussion

The purpose of developing methods for detecting electrode placement and recording artifacts is to improve the validity and reliability of the resulting EEG topographies. The intrinsic Hjorth provides a simple means for identifying bridged electrodes that is sufficiently unambiguous to be evident even to untrained individuals. This method is effective regardless of the relative locations and physical distances of the bridged pair, or the EEG recording reference. Since knowledge about existing electrolyte bridges or equipment-related electrical shorts is a prerequisite to successfully deal with problems arising from these artifacts, the intrinsic Hjorth is recommended as a routine screening procedure for ERP data.

The noise properties of the recording environment influence the effectiveness of the intrinsic Hjorth for detecting bridges. While ERP waveforms are, to some degree, protected against unsystematic noise by the averaging

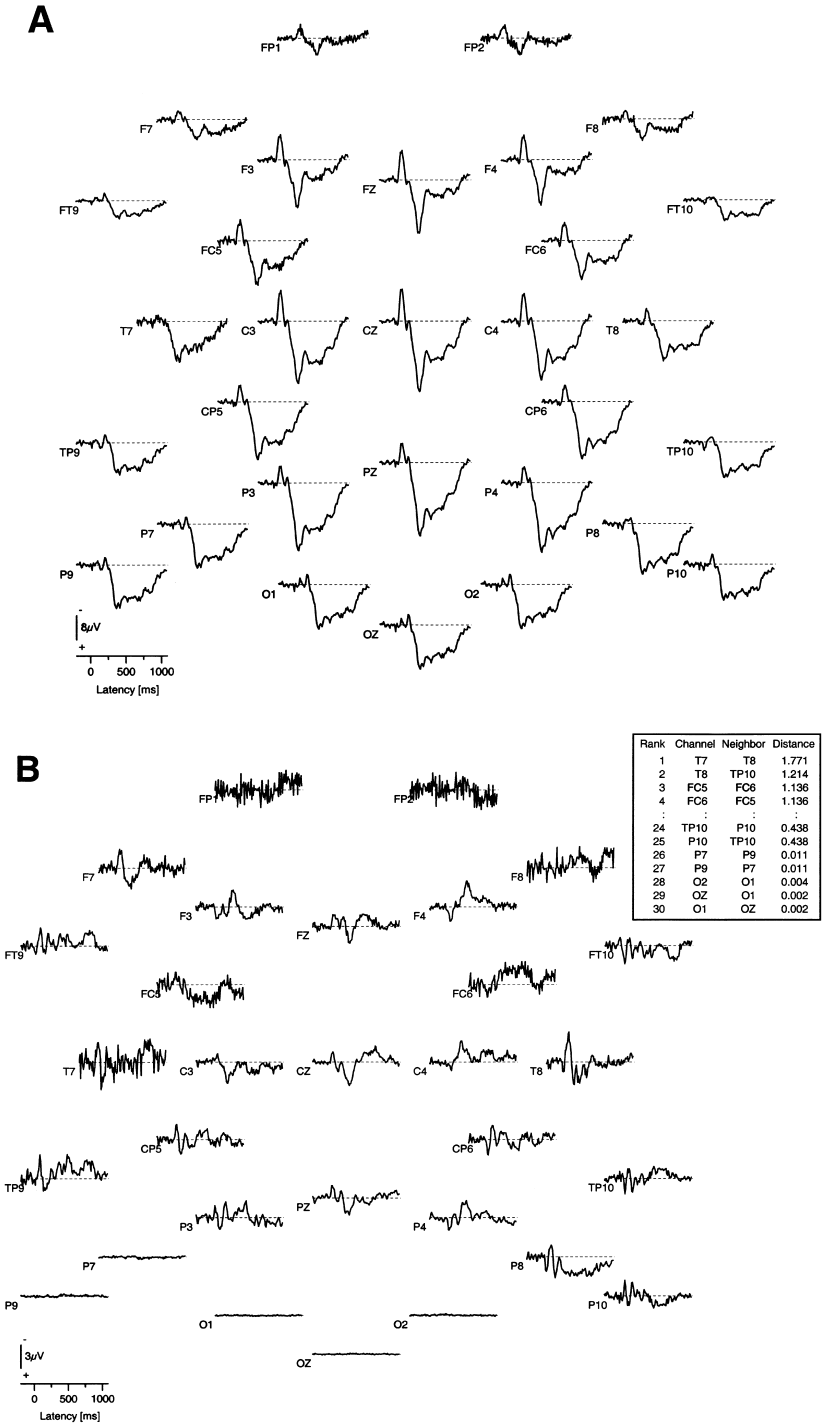

Rank	Channel	Neighbor	Distance
1	T7	T8	1.771
2	T8	TP10	1.214
3	FC5	FC6	1.136
4	FC6	FC5	1.136
:	:	:	:
24	TP10	P10	0.438
25	P10	TP10	0.438
26	P7	P9	0.011
27	P9	P7	0.011
28	O2	O1	0.004
29	OZ	O1	0.002
30	O1	OZ	0.002

Fig. 1. (A) Event-related potential (ERP) waveforms for one individual at 30 Electro-Cap recording sites for 60 tonal targets recorded during auditory oddball tasks with a nose reference (e.g. Tenke et al., 1998). Electrolyte bridges, which were created between electrode sites P7 and P9 over the left inferior-lateral hemisphere, and between occipital sites O1, Oz, and O2, resulted in nearly identical waveforms among linked sites, that are not immediately evident by visual inspection. (B) Corresponding intrinsic Hjorth waveforms computed for the single nearest electrical neighbor, in which linked electrode sites are characterized by distinct straight lines approximating zero. For each electrode, electrical distances to all other electrodes are computed, and the lowest value determines the nearest electrical neighbor. The inset table ranks electrodes (channels) and their nearest electrical neighbors by their electrical distance.

process, individual EEG epochs are particularly susceptible to machine noise, amplifier drift, and signal variability subsequent to amplifier saturation. Since even a minimal, mathematically simulated drift may degrade D_{i-j} estimates (cf. sites 43/99 in Fig. 2B), a spurious drift of relatively low amplitude confined to one of an otherwise highly similar pair of ERP waveforms (e.g. sites 56/63 in Fig. 2B) could mask their similarity. As a protective measure, and for the

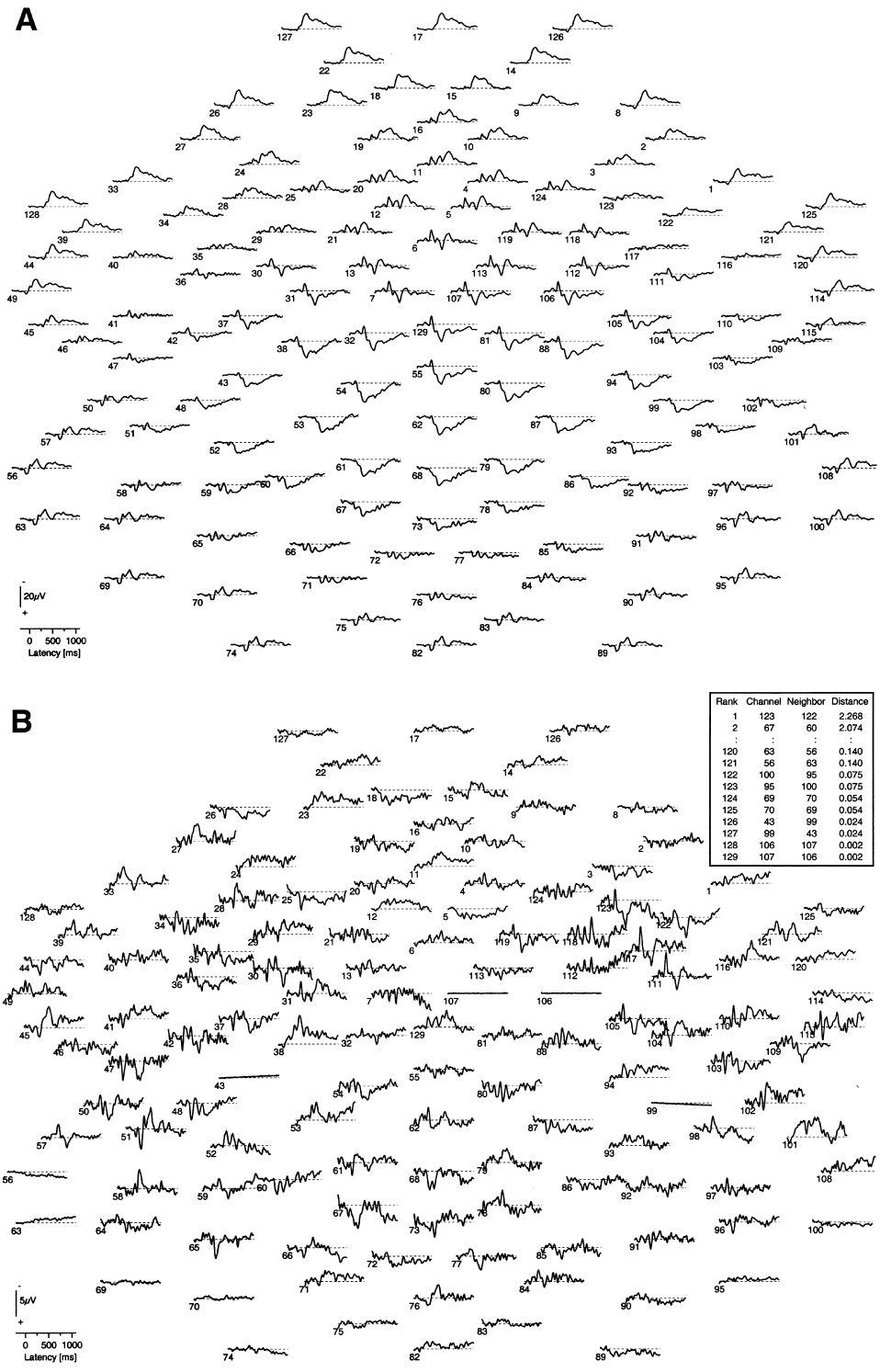

Fig. 2. (A) Event-related potential (ERP) waveforms for one individual at 129 Sensor Net recording sites for 61 tonal targets using an average reference (channel 129 corresponds to vertex site Cz). The two simulated bridges, which were inserted between two adjacent electrodes (right central sites 106 and 107) and two distant electrodes (left and right medial parietal sites 43 and 99), resulted in nearly identical waveforms at these sites and would go undetected by visual inspection. (B) The corresponding linked electrodes sites are identified with the intrinsic Hjorth (single nearest electrical neighbor) by distinct straight lines approximating zero, and low electrical distance values (see inset table). Similar flat lines, associated with somewhat larger electrical distance values, are also evident at left (i.e. 56/63, and 69/70) and right (i.e. 95/100) inferior-lateral sites, and may indicate the presence of physical electrolyte bridges in areas where excessive electrolyte had been applied.

sole purpose of enhancing the reliability of the D_{i-j} measure, waveforms could be linearly detrended first. This approach may then be developed into an automated bridge detection procedure based on empirically established thresholds for D_{i-j}.

Apart from the usefulness of this method for off-line screening of previously recorded ERP averages, it may also be used to ensure the absence of bridges prior to data collection. However, it must be noted that bridges may appear or disappear during the recording session, with an incidence rate and time course that will vary across recording systems. Although it would also be possible to measure electrical distances *during* data acquisition, it would apparently be necessary to accumulate averages across small blocks of test data to compensate for noise, thereby making bridges more distinct. While this technical note elaborated on applications for time-locked ERP averages, preliminary investigations using EEG amplitude spectra suggest that the intrinsic Hjorth may be equally applicable to these data for detecting bridged electrodes, provided filtering and detrending were applied to the EEG epochs before computing the frequency spectra.

While it is beyond the scope of this paper to elaborate on strategies for dealing with data recorded using one or more bridged pairs of electrode, it should be noted that they range from excluding affected averages, blocks, or individuals, to replacing data recorded at affected sites with interpolations from unaffected electrodes (a common strategy for large montages, e.g. Junghöfer et al., 1997). If it has been established that the introduced error is small and unsystematic, an informed decision may be made about the inclusion of affected averages based on the overall objective of the study.

Acknowledgements

This work was supported in part by grants MH058346 and MH36295. We thank research assistants in training for providing the data that brought our attention to the need for detecting electrolyte bridges in EEG/ERP recordings. We also thank Charles L. Brown for ERP display software.

References

Gevins A. High resolution evoked potentials of cognition. Brain Topogr 1996;8:189–199.

Hjorth B. Source derivation simplifies topographical EEG interpretation. Am J EEG Technol 1980;20:121–132.

Junghöfer M, Elbert T, Leiderer P, Berg P, Rockstroh B. Mapping EEG-potentials on the surface of the brain: a strategy for uncovering cortical sources. Brain Topogr 1997;9(3):203–217.

Kayser J, Tenke CE, Bhattacharya N, Stuart BK, Hudson J, Bruder GE. A direct comparison of Geodesic Sensor Net (128-channel) and conventional (30-channel) ERPs in tonal and phonetic oddball tasks. Psychophysiology 2000;37:S17.

Mitzdorf U. Current source-density method and application in cat cerebral cortex: investigation of evoked potentials and EEG phenomena. Physiol Rev 1985;65(1):37–100.

NeuroScan, Inc. SCAN Manual II Version 3.0. Herndon, VA; 1993.

NeuroScan, Inc. Intrinsic Hjorth transform. SCAN 3.0 technical note (http://www.neuro.com/neuroscan/hjorth.htm). Herndon, VA; 1995.

Pellouchoud E, Leong H, Gevins A. Implications of electrolyte dispersion for high resolution EEG methods. Electroenceph clin Neurophysiol 1997;102:261–263.

Perrin F, Pernier J, Bertrand O, Echallier JF. Spherical splines for scalp potential and current density mapping. Electroenceph clin Neurophysiol 1989;72:184–187.

Picton TW, Bentin S, Berg P, Donchin E, Hillyard SA, Johnson R, et al. Guidelines for using human event-related potentials to study cognition: recording standards and publication criteria. Psychophysiology 2000;37(2):127–152.

Tenke CE, Kayser J, Fong R, Leite P, Towey JP, Bruder GE. Response and stimulus-related ERP asymmetries in a tonal oddball task: a Laplacian analysis. Brain Topogr 1998;10(3):201–210.

Tucker DM. Spatial sampling of head electrical fields: the geodesic sensor net. Electroenceph clin Neurophysiol 1993;87:154–163.